# Polymer based carbons as potential materials for energy storage in Lithium /Oxygen batteries

***Mojtaba Mirzaeian [a] and Peter J Hall [b]***

*Department of Chemical and Process Engineering, University of Strathclyde, Glasgow, G1 1XJ, Scotland, UK*

**Abstract:** Porous carbon aerogels are prepared by polycondensation of resorcinol (R) and formaldehyde (F) catalyzed by sodium carbonate (C) followed by carbonization of the resultant aerogels at 800 ˚C in an inert atmosphere. The porous texture of the carbons has been adjusted by the change of the molar ratio of resorcinol to catalyst (R/C) in the gel precursors in the range of 100 to 500. The porous structure of the aerogels and carbon aerogels are characterized by $N_2$ adsorption-desorption measurements at 77 K. It is found that total pore volume and average pore diameter of the carbons increase with increase in the R/C ratio of the gel precursors. The prepared carbon aerogels are used as active materials in fabrication of composite carbon electrodes. The electrochemical performance of the electrodes has been tested by using them as cathodes in a $Li/O_2$ cell. Through the galvanostatic charge/discharge measurements, it is found that with an increase of R/C ratio, the specific capacity of the $Li/O_2$ cell fabricated from the carbon aerogels increases from 716 to 2077 mA h $g^{-1}$. The resulting voltage profiles for the first ten charge/discharge cycles indicate that the carbon samples possess excellent stability on cycling.

**Key words:** Rechargeable battery, lithium, oxygen, carbon, porosity, capacity.

[a] E-mail address: mojtaba.mirzaeian@strath.ac.uk ; Tel: +44 -141-5482075
[b] E-mail address: p.j.hall@strath.ac.uk ; Tel: +44 -141-5484084

# 1 Introduction

Increasingly global warming due to carbon emission is causing an energy revolution by requiring fossil fuels to be supplemented by alternative energy sources and by requiring changes in lifestyle. Thus the future energy landscape foresees a reduction in the use of fossil fuels by exploiting renewable energies as key energy supplies. Addressed to this need for environmental protection, there is extensive interest in the use of renewable energies and development of improved methods for energy storage to ensure the continuity of supply. To satisfy the critical demand for energy storage, it is essential to develop storage technologies that are capable of storing and delivering energy with longer service life as well as higher energy and power densities.

Due to their high energy density, high specific energy and high operating voltage, rechargeable lithium batteries are expected as the potential power sources for many applications such as consumer electronics and electric vehicles (EV) [1]. Lithium is an extremely light metal and has the lowest electronegativity of the standard cell potential -3.045 V in the existing metals [2]. It can donate electrons the most easily to form positive ions [3]. Commercial rechargeable lithium batteries use lithium transition metal oxides, typically $LiCoO_2$, as cathode and graphite as anode [4]. Their specific capacity depends on the capacities of both the cathode and anode materials. Graphite has a theoretical capacity of 372 mA h $g^{-1}$ [5]. Energy storage in these batteries is limited by the cathode and does not exceed 200 mA h $g^{-1}$ [6].

The capacity of a lithium battery system can be enhanced remarkably by using a completely different approach which combines Li as anode directly with oxygen as cathode active material in a Li/oxygen cell [6, 7]. Oxygen accessed from environment is reduced catalytically on an air electrode surface to form either an oxide or peroxide ion.

The catalytically formed anions react with lithium cations supplied by the anode and delivered by the electrolyte to form $Li_2O_2$ on the air electrode surface during discharge process. Oxygen the unlimited cathode active material is not stored in the battery and therefore the theoretical specific energy of the lithium/ oxygen battery (11400 W h $kg^{-1}$ excluded oxygen and 5200 W h $kg^{-1}$ included oxygen) is the highest among various metal/oxygen batteries and is still much larger than that achievable using a conventional lithium ion battery [7].

The $O_2$ electrode in lithium/oxygen batteries is a carbon having a porous structure in which several electrochemical and transport processes occur simultaneously. The porous structure acts as gas transport pores for the diffusion of oxygen to the carbon-electrolyte interface (reaction zoon), formation and storage of $Li_2O_2$ during the discharge process and also electrochemical decomposition of $Li_2O_2$ during the charge process. The Kinetics of oxygen diffusion through the cathode limits the performance of the Li/oxygen cells [8]. It has been also discussed that the end-of-discharge of the cell is reached when the carbon pores are filled or choked by the deposition of $Li_2O_2$ [6, 9]. This shows that the cell performance strongly depends on the morphology and structure of the carbon. Therefore the main challenge in this issue is the development of new carbon electrode materials to improve the kinetics of the air cathode and enhance the capacity, energy and power densities and the stability of the energy delivered by these systems.

In this work we aim to prepare high capacity electrodes based on R-F carbon aerogels as cathode electrode for $Li/O_2$ batteries. The porous structures of the carbons are discussed with emphasize on the synthesis routes and porosity and surface area

measurements. The electrochemical performance of the carbon aerogel electrodes are examined by galvanostatic charge / discharge tests using a Solartron 1470 equipment.

## 2 Experimental

### 2.1 Chemicals

Resorcinol [$C_6H_4$ $(OH)_2$, Sigma- Aldrich, 98% ], formaldehyde [(HCHO), Sigma-Aldrich, 37% solution ], sodium carbonate anhydrous [$Na_2CO_3$, Sigma- Aldrich, ≥ 99.5% ], acetone [ Fisher Scientific, reagent grade ], lithium hexafluorophosphate [ $LiPF_6$, Sigma- Aldrich, ≥ 99.99 % (battery grade)], lithium ribbon [ Li, Sigma- Aldrich, 99.9% ], Propylene carbonate anhydrous [ $C_4H_6O_3$, Sigma- Aldrich, 99.7%]

### 2.2 R-F aerogel synthesis

R-F hydrogels were synthesized by polycondensation of resorcinol [$C_6H_4$ $(OH)_2$ ] (R) with formaldehyde [HCHO] (F) according to the method proposed by Pekala et al [10,11]. R-F solutions were prepared by mixing the required amount of resorcinol (R), formaldehyde (F), sodium carbonate (C) and distilled water (W) under vigorous stirring for 45 minutes. The homogeneous R-F solutions were poured into sealed glass vials to prevent the evaporation of water during gelation and gelled by aging for 72 hours at 90 ˚C into an oven to obtain R-F hydrogels. The hydrogels have a structure filled with water. To remove water from their structure, the gels were solvent exchanged by immersing into acetone for several hours prior to the vacuum drying. Finally the

hydrogels were dried in a vacuum oven at 80 ˚C for 3 days. R-F aerogels with different resorcinol to catalyst (R/C) ratios were prepared by this method.

### 2.3 Preparation of carbon aerogels

Carbonization of the resultant R-F aerogels was performed at 800 ˚C in a tubular furnace using the following method: Typically 3 grams of gel was used in each carbonization experiment. The gel was placed in a ceramic boat and purge with Ar flowing at 200 ml $min^{-1}$ for 30 min at room temperature prior to the heating program. The furnace was heated to 150 ˚C at 5 ˚C $min^{-1}$ and maintained at 150 ˚C for 30 min. Then it was heated to 400 ˚C at 5 ˚C $min^{-1}$ and hold for 30 min. Finally it was heated to the carbonization temperature at 10 ˚C $min^{-1}$ and kept for 3 hours. The whole heating program was performed under Ar flowing at 200 ml $min^{-1}$. After pyrolysis, the furnace was cooled in flowing Ar to room temperature.

### 2.4 Material characterization

The pore texture of dried gel and carbon materials were studied by the analysis of nitrogen adsorption-desorption isotherms measured by an ASAP 2000 adsorption analyzer (Micromeritics) at 77 K. The samples were evacuated at 373 K for 2 h prior to the adsorption measurements. BET method was used for surface area measurements, BJH adsorptions-desorption was used for mesopore analysis and t-plot method was used for micropore analysis. Total pore volume was calculated from the adsorbed volume of nitrogen at $P/P_0 = 0.99$ (saturation pressure). Pore size distributions were obtained by the BJH method from adsorption branch of the isotherms.

## 2.5 Cell construction and electrochemical measurements

Cathode electrodes were prepared by mixing porous carbon-aerogel sample, electrolytic manganese dioxide (EMD), Kynar Flex 2801 binder (polyvinylidene difluoride/hexafluoropropylene; PVDF/HFP 88/12 by weight) and propylene carbonate (PC) (weight ratios: 11/19/15/55) according to the procedure described elsewhere [7,9]. The materials are placed in a glass bottle to which acetone and a stirrer bar are added and the resulting mixture was left to stir for 4 hours to form a paste. Then the paste was spread into a 200 μm thick film by an applicator. The electrode was untouched until the acetone evaporates. Disks of 1.3 cm diameter were then cut to make disk-like cathode electrodes.

Electrochemical cell was constructed in an argon-filled glove box. The cell consists of a stainless still bar as anode current collector, a lithium metal foil as anode, a glass micro-fiber separator soaked with electrolyte (1 M LiPF6 in propylene carbonate), a cathode electrode, an aluminum mesh and a spring and a hollow aluminum bar on the top of it as cathode current collector. The cell parts were compressed together to ensure that the electrode contact is good and then the cell was completely sealed except for the Al mesh window that exposes the porous cathode to the $O_2$ atmosphere. The cell then was exposed to $O_2$ at atmospheric pressure for a minimum of 30 min prior to the electrochemical tests and all measurements were carried out under $O_2$ atmosphere at room temperature.

Galvanostatic charge/discharge tests were performed by a Solartron 1470 potentiostat by applying a constant current at charge/discharge rate of 50 mA $g^{-1}$ in the voltage range between 2 and 4.5 V.

## 3 Results and discussion

### 3.1 Surface characterization of aerogel samples

Adsorption-desorption isotherms of aerogels prepared at various R/C ratios are shown in Figure 1. The adsorption-desorption isotherms for sample having R/C ratio of 200 show significant hysteresis loop with type-IV isotherm which is representative of the filling and emptying of mesopores in the $P/P_0$ region of 0.4 - 0.85 by capillary condensation of the adsorbate in the mesopores of the solid [12]. This suggests the mesoporosity in the solid [12, 13]. The lower part of the hysteresis loop represents the filling of the mesopores while the upper part represents the emptying of the mesopores.

In the case of RF003 sample with R/C = 500 the hysteresis loop is shifted to the higher relative pressures (i.e. $P/P_0$ region of 0.75 - 0.99) indicating the emptying and filling of wider pores. For RF001 sample with R/C = 100 adsorption-desorption isotherms show a small hysteresis loop in the $P/P_0$ region of 0.4 - 0.6.

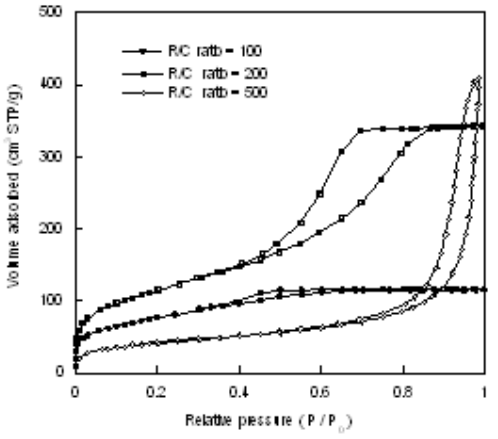


**Figure 1**. $N_2$ adsorption-desorption isotherms at 77 K for R-F aerogels prepared at various R/C ratios.

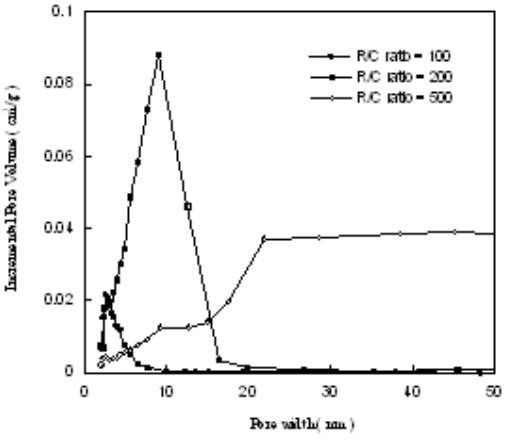


**Figure 2**. Pore size distribution of R-F aerogels with different R/C ratios.

**Table 1. Surface characterization of R-F aerogel samples prepared at various R/C ratios**

| Sample | R/F | R/C | R/W | $S_{BET}$ $m^2/g$ | $V_{total}$ $cm^3/g$ | $V_{micro}$ $cm^3/g$ | $V_{meso}$ $cm^3/g$ | $\%V_{micro}$ | $\%V_{meso}$ | $D_{avg}$ nm |
|---|---|---|---|---|---|---|---|---|---|---|
| RF001 | 0.50 | 100 | 0.1 | 278 | 0.1797 | 0.1189 | 0.0608 | 66.16 | 33.83 | 2.58 |
| RF002 | 0.50 | 200 | 0.1 | 417 | 0.5301 | 0.1801 | 0.350 | 33.44 | 66.56 | 5.10 |
| RF003 | 0.50 | 500 | 0.1 | 149 | 0.632 | 0.0075 | 0.6245 | 1.186 | 98.814 | 16.96 |

From data for the isotherms of the R-F aerogels, surface area, pore volume, and pore size distribution were calculated. The pore size distribution was calculated using the BJH method. The micro pore volume was calculated using t-plot method and mesopore volume was determined by difference. The above mentioned characteristics of the R-F aerogels are shown in Figure 2 and Table1. Data given in Table 1 show that increasing R/C ratio, increases total pore volume and level of mesoporosity in aerogels.

### 3.2 Effect of carbonization on the porous structure of the gels

Figure 3 shows adsorption and desorption isotherms of nitrogen on aerogel RF001 and carbon-aerogels CRF001 prepared at different carbonization temperatures.

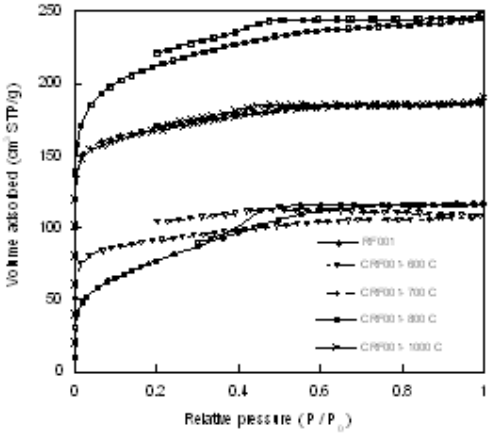


**Figure 3**. $N_2$ adsorption-desorption isotherms at 77 K for RF001 aerogel and CRF001 carbon-aerogels.

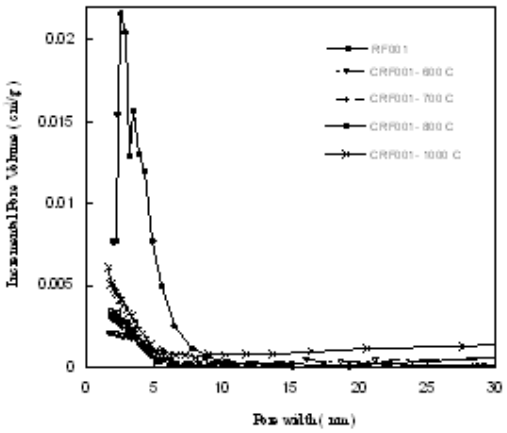


**Figure 4**. Pore size distribution of RF001 aerogel and CRF001 carbon-aerogels.

This figure suggests that the amounts of nitrogen adsorbed by carbon aerogels increases with increase in the carbonization temperature for T ≤ 800 ˚C. The results mean that porosity of carbon gels increases with increasing temperature in this range. As carbonization temperature increases to 800 ˚C, carbonization modifies the porous structure of the original gel and creates more micropores in the structure. This can be observed by a sharp rise at the initial region of the isotherm with temperature (i.e. at low relative pressures) which is indicative of the presence of micropores in carbon aerogels.

Figure 3 also shows that for carbonization temperatures above 800 ˚C, the amounts of nitrogen adsorbed by carbon aerogels decreases with increase in temperature which means decrease in the porosity of the carbon aerogel with increase in the carbonization temperature probably due to the collapse of the porous structure at high temperatures. Changes in the pore parameters of the carbon aerogels with heat treatment temperatures are listed in Table 2. Data shows that both total surface area and total pore volume increase with carbonization temperature for carbon aerogels below 800 ˚C. Heat treatment of carbon aerogel above 800 ˚C was found to decrease both total surface area and pore volume.

**Table 2. Surface characterization of the aerogel and carbon aerogels prepared at various temperaments**

| Sample | Temperature (˚C) | $S_{BET}$ $m^2/g$ | $V_{total}$ $cm^3/g$ | $V_{micro}$ $cm^3/g$ | $V_{meso}$ $cm^3/g$ | $\%V_{micro}$ | $\%V_{meso}$ | $D_{avg}$ nm |
|---|---|---|---|---|---|---|---|---|
| RF001 | - | 278 | 0.1797 | 0.1189 | 0.0608 | 66 | 34 | 2.5830 |
| CRF001-600 | 600 | 286 | 0.1870 | 0.1484 | 0.0386 | 79 | 21 | 2.3351 |
| CRF001-700 | 700 | 524 | 0.2874 | 0.2625 | 0.0249 | 91 | 9 | 2.2708 |
| CRF001-800 | 800 | 669 | 0.3800 | 0.3300 | 0.0500 | 86 | 14 | 2.1938 |
| CRF001-1000 | 1000 | 520 | 0.2905 | 0.2603 | 0.0302 | 89 | 11 | 2.2316 |

Figure 4 shows the pore size distributions of the aerogel and carbon aerogels prepared at different temperatures. There is a significant change in mesopore size distribution of the gel after carbonization. Pore size distribution curves show that carbonization process decreases volume of pores significantly for pores with diameter in the range of 3 to 10 nm. Data given in Table 2 suggests that decrease in the mesoprosity of the gel is in expense of increase in microporosity during carbonization process as the total pore volume increases with heat treatment.

### 3.3 Surface characterization of carbon aerogels

Adsorption-desorption isotherms of nitrogen at 77 K for carbons prepared form aerogels with different R/C ratios at 800 ˚C are shown in Figure 5. The adsorption-desorption isotherms for CRF001 carbon aerogel (R/C = 100) show a type I isotherm according to IUPAC, indicating that this sample is microporous [12, 13]. The initial part of isotherm shows micropore filling and the low slop of the plateau is due to multilayer adsorption on the external surface.

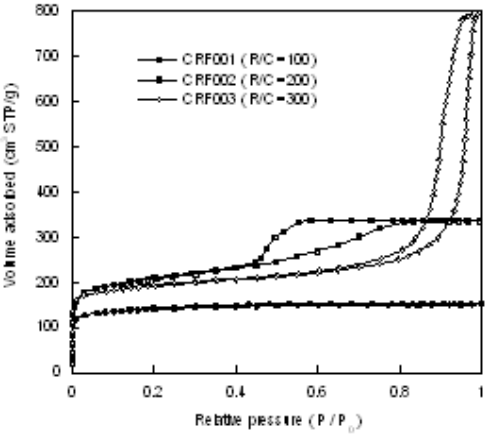


**Figure 5**. $N_2$ adsorption-desorption isotherms at 77 K for carbon-aerogels with different R/C ratios.

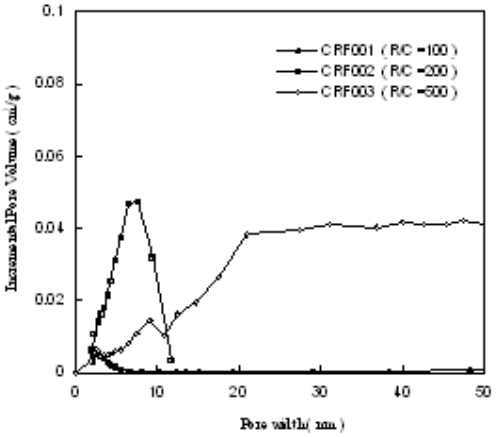


**Figure 6**. Pore size distribution of carbon-aerogels with different R/C ratios.

This shows that carbonization introduces large quantity of micropores into the carbon structure. For CRF002 sample (R/C = 200) the initial region of the isotherms (i.e. at low relative pressures: 0 – 0.2) experience a sharp rise which is indicative of the presence of micropores in the sample. Hysteresis loop in the pressure range 0.4 - 0.8 is indicative of mesoporosity in the structure of the carbon in addition to the presence of micropores. In the case of CRF003 sample (R/C = 500) hysteresis loop for filling and emptying of mesopores is shifted to a higher pressure range (i.e. 0.7 – 1.0) which is associated with the presence of mesopores with larger size in the structure. Pore size distribution of the carbon samples are shown in Figure 6. Sample CRF001 exhibits a micropore peak at the pore width of 2 nm and there is a shift of pore width to 7.8 nm and 20.9 nm for CRF002 and CRF003 samples respectively. The porous textural parameters, such as specific surface area, pore volume and average pore diameter for carbon samples are listed in Table 3.

**Table 3. Porous textural parameters of carbon samples**

| Sample | R/C | $S_{BET}$ $m^2/g$ | $V_{total}$ $cm^3/g$ | $V_{micro}$ $cm^3/g$ | $V_{meso}$ $cm^3/g$ | $\%V_{micro}$ | $\%V_{meso}$ | $D_{avg}$ nm |
|---|---|---|---|---|---|---|---|---|
| CRF001 | 100 | 669 | 0.3800 | 0.3300 | 0.0500 | 86.84 | 13.16 | 2.1938 |
| CRF002 | 200 | 707 | 0.5270 | 0.1884 | 0.3386 | 35.75 | 64.25 | 4.4234 |
| CRF003 | 500 | 647 | 1.2245 | 0.2101 | 1.0144 | 17.16 | 82.84 | 21.6503 |

It can be observed that with increase of the mole ratio of R/C in the initial gels both the total pore volume and the average pore diameter of the resultant carbons increase from 0.38 to1.2245 $cm^3$ $g^{-1}$ and 2.1938 to 21.6503 nm, respectively. Three carbons prepared in this work possess different porous structures ranging from microporous structure, small mesopore in the structure and large mesopore in the structure. These results indicate that the porous texture and specially the pore volume and the pore size

distribution of the carbon materials can be adjusted by changing the R/C ratio of the gel precursors. Pores in carbon electrode allow both the oxygen gas and electrolyte to come in contact with the catalyst and carbon. The electrochemical reduction of oxygen takes place on the carbon surface. Therefore it is important to minimize diffusion barriers to increase storage capacity of $Li/O_2$ cells by tailoring carbon electrodes having appropriate porous textures and pore volumes that maximize electrolyte and oxygen accessibility to the porous network. Electrochemical performance of cathode electrodes made from the above mentioned carbons are studied in order to find high capacity carbon based electrodes for lithium/oxygen cells.

### 3.4 Electrochemical studies

All the data reported below are obtained from the galvanostatic charge/discharge cycling of the cells assembled as described above. Assuming that the products of the discharge reaction in $Li/O_2$ cell deposit only onto carbon, the charge/discharge capacity of the lithium/oxygen cells has been normalized to the weight of carbon in the cathode electrode.

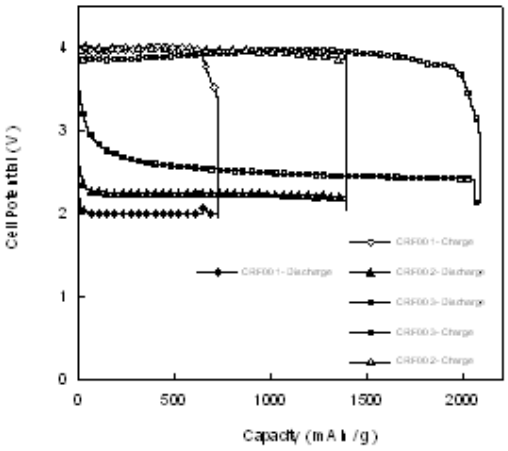


**Figure 7**. Discharge/charge behavior of the $Li/O_2$ cell at 50 mA $g^{-1}$ based on electrodes prepared from CRF001, CRF002 and CRF003 carbons

Figure 7 shows a plot of charge/discharge characteristics of the $Li/O_2$ cells (third cycles) based on electrodes prepared from CRF001, CRF002 and CRF003 carbons. Variations of Cell voltage are plotted against specific capacity of the active material (carbon) when cells were charged and discharged at constant current rate of 50 mA $g^{-1}$.

Three carbon samples show flat discharge and charge profiles ranging between 2 to 2.5V and 3.85 to 4.05 respectively. These are associated with the storage behavior of the cells and are in good agreement with the preceding reported data for a similar cell discharged in $O_2$ at atmospheric pressure involving formation of $Li_2O_2$ as discharge product [6, 7]. Results of cyclic discharge/charge testing of carbon samples are given in Table 4.

**Table 4. Results of galvanostatic discharge/charge testing of carbon samples**

| Sample | Charge voltage ( V ) | Discharge voltage ( V ) | Average reversible capacity ( mA.h/g ) |
|---|---|---|---|
| CRF001 | 3.97 | 2.0 | 716 |
| CRF002 | 4.05 | 2.2 | 1381 |
| CRF003 | 3.85 | 2.5 | 2077 |

Data given in Table 4 show that type of carbon used in cathode electrode has a significant effect on discharge capacity at 50 mA $g^{-1}$. CRF003 sample with the highest pore volume shows the highest discharge capacity (2077 mA h $g^{-1}$) while CRF001 sample with the lowest pore volume has the lowest discharge capacity (716 mA h $g^{-1}$) between carbon samples. The discharge reaction at the cathode results in the deposition of $Li_2O_2$ or $Li_2O$ on the surface and pores of the carbon based cathode. Discharge ends when the cathode is choked off with deposit and all of the pores in the electrode are filled [6]. It is presumed that porous structure of carbon is the main factor controlling termination of discharge process and affecting the capacity of the cell. As discharge

process proceeds, $Li_2O_2$ forms and fills pores in the carbon structure. If the porous structure is dominated by micropores, formation of discharge products chocks off micropores and significant fraction of the porous structure may not be electrochemically accessible which results in a small capacity for the cell. This is what has happened in a cell using CRF001 sample as active material in the cathode. When the R/C ratio increases to 500, the average reversible capacity increases to 2077 mA h $g^{-1}$ the highest value in all samples. The large discharge capacity of CRF003 carbon might be due to the appropriate fraction of mesopres formed during the gelation and carbonization processes.

Mesopores are important for improving the performance of $Li/O_2$ cells. They lead the electrolyte ions transport into the bulk of material quickly and provide larger space for formation of discharge products. Therefore for a sample with wider pores and larger pore volume, polarization due to the formation of solid $Li_2O_2$ in pores is less and consequently larger discharge capacity is obtained.

Associating the reversible capacity with the textural parameters of the porous carbon materials shows that appropriate pore volume and average pore diameter are key factors contributing to high capacity. This increased capacity might be due to the contributions of higher diffusivity of the electrolyte into the carbon structure which results in the better transport and accessibility of lithium ions to the carbon surface (reaction zoon), larger space for the storage of discharge products as larger pore volume is available in the porous structure, and finally better diffusion of oxygen to the carbon-electrolyte interface. Change in the conductivity of the cathode with its pore volume is an important issue in the performance of $Li/O_2$ batteries which needs to be studied.

One of the vital characteristics of a rechargeable cell is the ability to accept repeated charge/discharge cycles without significant performance deterioration. The resulting voltage profiles for the first ten charge/discharge cycles for cycling of $Li/O_2$ cells using CRF001 and CRF003 as active materials between 2 and 4.5 V at 50 mA $g^{-1}$ are shown in Figures 8-9.

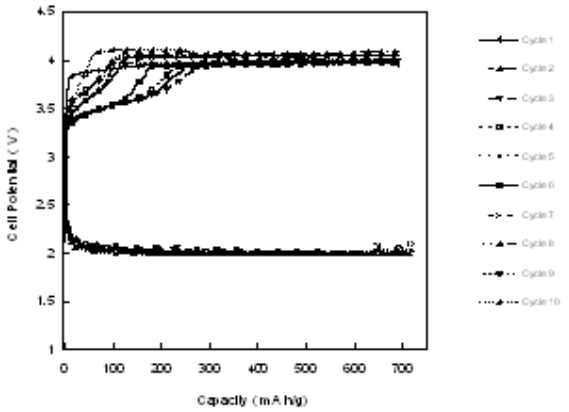


**Figure 8**. First ten charge/discharge curves for CRF001 carbon at 50 mA $g^{-1}$.

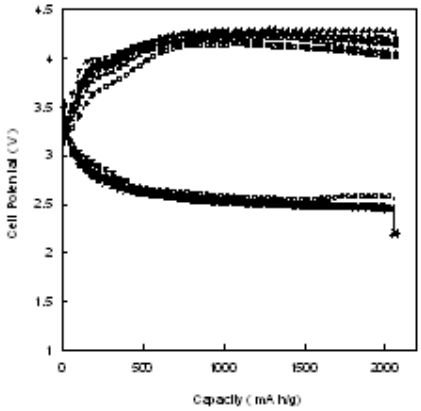


**Figure 9**. First ten charge/discharge curves for CRF003 carbon at 50 mA $g^{-1}$.

Charge/discharge cycles show that CRF001 and CRF003 based electrodes possess good cycling efficiencies and specific reversible capacities at these current density and voltage range.

## 4 Conclusions

Porous R-F gels have been synthesized through polycondensation of resorcinol with formaldehyde catalyzed by sodium carbonate. The porosity of the final gel is adjusted by changing the molar ratio of resorcinol to formaldehyde in the range of 100 to 500. The gels are used as precursors to prepare porous carbon materials with controlled porous

structure by carbonization at 800 ˚C in an inert atmosphere. With an increase of R/C ratio from 100 to 500, both the total pore volume and average pore diameter of the carbons increased from 0.38 to1.2245 $cm^3$ $g^{-1}$ and 2.1938 to 21.6503 nm, respectively. These porous carbon materials are investigated as active materials in cathode electrodes for $Li/O_2$ batteries and their electrochemical behavior has been characterized by constant current charge/discharge experiments. The results of electrochemical measurements show that with an increase of R/C ratio in carbon precursors from 100 to 500, the specific capacity of the $Li/O_2$ cell fabricated from the resultant carbons increases from 716 to 2077 mA h $g^{-1}$. The resulting voltage profiles for the first ten charge/discharge cycles indicate that the carbon samples sustain excellent stability on cycling.

**Acknowledgments**

We thank the EPSRC for funding as part of the Supergen Energy Storage Consortium (grant code EP/D031672/1).

**References**

[1] D. Linden, B. T. Reddy, Hand book of batteries, 3rd ed., McGraw-Hill, New York, 1989.

[2] M. Endo, C. Kim, K. Nishimura, Fujino T, K. Miyashita, Carbon, 38 (2000) 183-197.

[3] JP. Gabano, Lithium batteries, Academic press, New York, 1983.

[4] S. Flandrois, B. Simon, Carbon, 37 (1999) 165-180.

[5] R. Yazami, Ph. Touzain, J. Power Sources, 9 (1983) 365.

[6] K. M. Abraham, Z. J. Jiang, J. Electrochem. Soc., 143 (1996) 1-5.

[7] T. Ogasawara, A. Debart, M. Holzapfel, P. Novak, P.G. Bruce, J. Am. Chem. Soc., 128 (2006)1390-1393.

[8] J. Read, K. Mutolo, M. Ervin, W. Behl, J. Wolfenstine, A. Driedger, D. foster, J. Electrochem. Soc., 150 (2003) A1351-A1356.

[9] J. Read, J. Electrochem. Soc., 149 (2002) A1190-A1195.

[10] R W. Pekala, J. Mat. Sci., 24 (1989) 322.

[11] R W. Pekala, W. Schaefer, Macromolecules, 26 (1993) 5487-5493.

[12] F. Rouquerol, J. Rouquerol, K. Sing, Adsorption by powders and porous solids, principles, methodology and applications, Academic Press, New York, 1999.

[13] S. J. Gregg, K. S. W. Sing, Adsorption, surface area and porosity, Academic Press, New York, 1967.